

FUNCTIONALLY GRADED COMPOSITES WITH VERTICALLY ALIGNED CARBON NANO-TUBE (VACNT) EMBEDDED LAYERS FOR ENERGY ABSORPTION

Prabhakar R. Mantena¹ and Veera M. Boddu²

¹Department of Mechanical Engineering,
University of Mississippi, University, MS 38677, USA
Email: meprm@olemiss.edu

²U. S. Army Engineer Research and Development Center
Construction Engineering Research Laboratory (ERDC-CERL)
Champaign, IL 61821, USA
Email: veera.boddu@usace.army.mil

Keywords: VACNT forest, Silicon wafer, Woven fiber-glass, Polyester, Polyurethane, Dynamic Mechanical Analysis, Split Hopkinson Pressure Bar (SHPB), High strain-rate energy absorption

ABSTRACT

In the initial phase of work reported here, straight vertically aligned carbon nanotube (VACNT) forest ensembles are grown on silicon wafer substrate at various temperatures; including 720, 770 and 820 °C. Flexural rigidity (storage modulus) and loss factor (damping) of the VACNT-Si wafer specimens were measured with a dynamic mechanical analyzer in an oscillatory three-point bending mode. A Split Hopkinson Pressure Bar (SHPB) was used for determining the dynamic response under high strain-rate compressive loading. In the second phase, dynamic mechanical behavior and energy absorption characteristics of nano-enhanced functionally graded composites; consisting of 3 layers of vertically aligned carbon nanotube (VACNT) forests grown on woven fiber-glass (FG) layer and embedded within 10 layers of woven FG, with polyester (PE) and polyurethane (PU) resin systems (FG/PE/VACNT and FG/PU/VACNT), are investigated and compared with the baseline materials, FG/PE and FG/PU (i.e. without VACNT).

1 Introduction

Nanometer-scale structures such as carbon nanotubes (CNTs) and nanowires with exceptional thermal, electronic and mechanical properties are undergoing intense experimental and theoretical investigations for a large range of possible applications. With the ready availability of freestanding VACNTs, integrating high flexural rigidity and damping into structures is feasible. Increasing the energy dissipation characteristics by introducing stiffness gradients through topological defects and entanglements of the CNTs will also be beneficial in designing shock and impact resistant light-weight protection systems. Development of novel, light-weight, high-strength, and high-temperature resistant materials has been the focus of increased research for many applications [1]; such as aerospace and automobile structures, where the material experiences severe thermal gradients, and requires high flexural rigidity and high vibration damping. Due to the increasing demand of required conflicting properties, the newly developed functionally graded materials (FGM) have been a broad research area on account of their tailored properties [2, 3]. Investigation of carbon nanotubes' (CNT) role in CNT-polymer composites and their dynamic behavior can also help to develop such FGM [4]. CNT can enhance the mechanical properties of FGM, due to their unique material properties, such as high stiffness, strength, and toughness [5, 6]. These nano-enhanced FGM are being considered for blast/ballistic protective structures and other armor applications. Zeng et al. [7] studied the mechanical properties of VACNT based sandwich composites

using DMA. It was observed that VACNT based sandwich composites showed higher flexural rigidity and damping compared to samples consisting of carbon fiber fabric stacks without VACNT.

In the first phase of work reported here, straight vertically aligned carbon nanotube (VACNT) forest ensembles are grown on silicon wafer substrate using the well established chemical vapor deposition (CVD) approach at various temperatures; including 720, 770 and 820 °C. Flexural rigidity (storage modulus) and loss factor (damping) of the VACNT-Si wafer specimens were measured with a dynamic mechanical analyzer in an oscillatory three-point bending mode. A Split Hokinson Pressure Bar (SHPB) was used for determining the dynamic response under high strain-rate compressive loading. In the second phase, dynamic mechanical behavior and energy absorption characteristics of nano-enhanced functionally graded composites; consisting of 3 layers of vertically aligned carbon nanotube (VACNT) forests grown on woven fiber-glass (FG) layer and embedded within 10 layers of woven FG, with polyester (PE) and polyurethane (PU) resin systems (FG/PE/VACNT and FG/PU/VACNT); are investigated and compared with the baseline materials FG/PE and FG/PU (i.e. without VACNT).

2 Materials and Test Methods

2.1 VACNT-Si Specimen Preparation: A well established Chemical Vapor Deposition approach [8 - 11] has been used for the synthesis of VACNTs on silicon wafers. The VACNT forests used in this study are grown using m-xylene as a source of carbon and ferrocene as the catalyst at various temperatures; including 720, 770 and 820 °C.

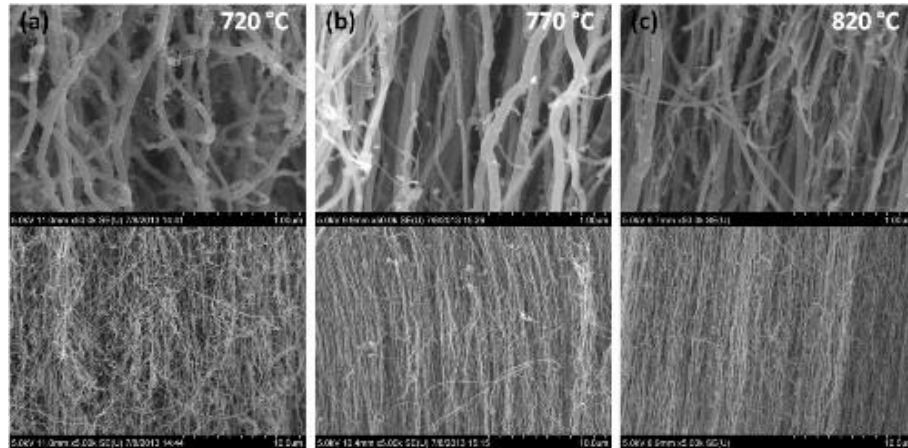


Figure 1: Multiwall VACNT forests synthesized using the chemical vapor deposition approach grown at (a) 720 °C, (b) 770 °C, and (c) 820 °C (shown at two different magnifications) [21].

Figure 1 shows scanning electron micrographs of the VACNT forests grown at these three temperatures, and at two different magnifications. It can clearly be observed that the vertical alignment increases with process temperature. However, some variation in the mechanical properties of these CNTs synthesized at different temperatures may be expected due to the thermal conditions these VACNTs were exposed to during the synthesis process.

2.2 Woven fiber-glass Composites with Embedded VACNT Layers Specimen Preparation: 10 layer woven FG fabrics with PE resin (E15-8082) and 10 layer woven FG fabrics with PU resin (3475 Urethane Casting) were prepared as baseline composites (FG/PE and FG/PU). Carbon nanotubes were grown on 12" by 12" sheet of desized glass fabric. Three sheets of the fabric were arranged on each of three racks in a steel chamber (18"x18"x9") which was heated to about 650 °C. A solution of 4% by wt. ferrocene in m-xylene was prepared to implement the floating catalyst fabrication of CNTs and fed through three inlet manifolds, each of which was externally heated to about 350 °C to vaporize the solution. Nitrogen and hydrogen, at a flow rate of 2000 and 300 cubic cm/min, respectively, carried the vapor into the reaction

chamber containing the glass fabrics. The fabrics were processed for 60 minutes. The temperature in the reaction chamber, however, fluctuated ($\pm 50^{\circ}\text{C}$) significantly around 600°C during the CNT growth process. A total ferrocene/catalyst solution of about 300-400 mL was used. FG/PE/VACNT and FG/PU/VACNT specimens having 3 layers of VACNT grown/embedded within 10 layers of woven FG along with two different resin systems (PE and PU) were fabricated, by hand lay-up and compression. More details of the specimen preparation and fabrication are given in [12]. A schematic of the FG/PE/VACNT and FG/PU/VACNT composites is shown in Figure 2.

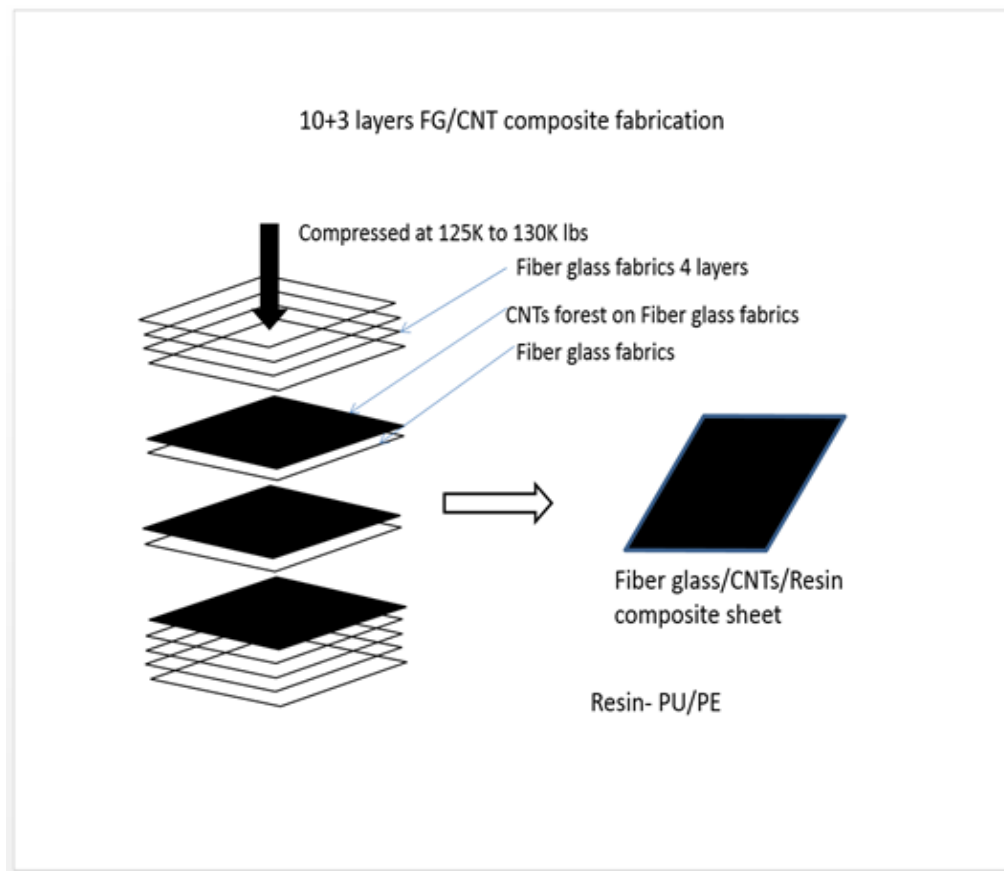


Figure 2: Schematic of FG/PE/VACNT and FG/PU/VACNT samples with 10 layers of woven fiber-glass + 3 layers of embedded VACNT [12].

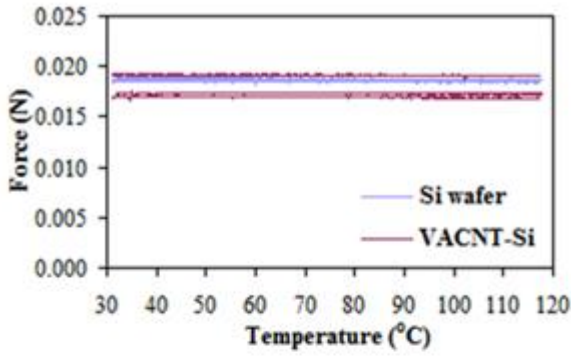
2.3. *Dynamic Mechanical Analysis*: The dynamic mechanical properties [7, 13] of pure Si wafer, VACNT-Si, FG/PE, FG/PU, FG/PE/VACNT and FG/PU/VACNT specimens were investigated using a *TA Instruments Model Q800 DMA* [14]. Rectangular beam specimens; 60 mm in length, 10 mm in width, and 6 mm in thickness, provided by ERDC-CERL [15] were used for this study. Mechanical properties such as storage modulus (flexural stiffness), loss modulus (energy dissipation), $\text{Tan } \delta$ (inherent damping), and glass transition temperature (T_g) were obtained in the three-point oscillatory bending mode. Roller pins on each side (with a span of 50 mm) were used to support the specimens, and force applied in the middle of the span. All the specimens were subjected to 1 Hz single frequency with 10 μm mid-span displacement amplitude. A temperature ramp from ambient (30°C) to 200°C was implemented, and the temperature was elevated with $2^{\circ}\text{C}/\text{min}$ steps up to the final temperature. Poisson's ratio of 0.3 is input as a constant parameter for all samples.

2.4 SHPB Compression Tests: High strain-rate compression tests were conducted on the pure Si wafer, VACNT-Si, FG/PE, FG/PU, FG/PE/VACNT, and FG/PU/VACNT specimens using a modified SHPB in the Blast and Impact Dynamics Lab at the University of Mississippi, MS. Aluminum bars of 19.02 mm diameter were used as striker, incident and transmission bars. Square specimens were cut precisely and tested with compression SHPB apparatus to evaluate the dynamic mechanical properties such as compressive strength, specific energy absorption, and rate of specific energy absorption. Polyurea pulse shaper was used to minimize the wave dispersion and for achieving the required stress equilibrium [16]. Glycerin was also used for holding specimens in between incident and transmission bar ends to minimize the interfacial friction.

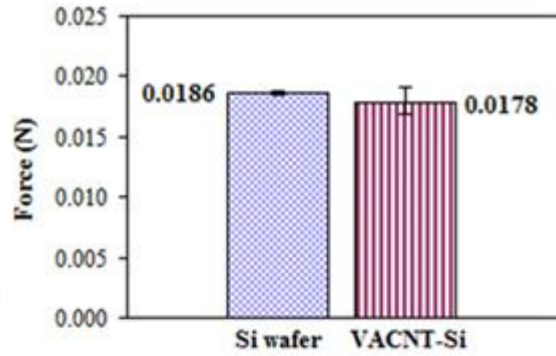
3 Results and Discussion

3.1.1 DMA Response of VACNT-Si Specimens: Three specimens each of pure Si wafer and VACNT-Si were tested in the DMA under three-point oscillatory flexural load over a temperature range from ambient (30 °C) to 120 °C. The flexural rigidity and damping of these specimens were investigated in terms of the required force (F , line force at mid-span to achieve 10 μm amplitude - Figures 3 (a) and (b)), 'apparent' storage modulus (E' - Figures 3 (c) and (d)), and the damping loss factor ($\tan\delta$, ratio of dissipated energy to stored energy - Figures 3 (e) and (f)).

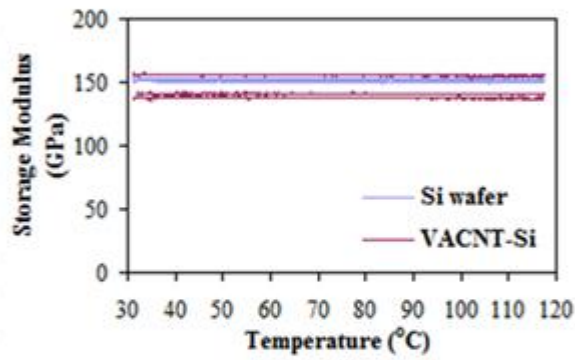
As can be observed, these values remain constant over the 120 °C test temperature range; without a demonstrated peak of loss factor along with drop in storage modulus, which is more typical for viscoelastic materials around their glass transition temperature [7, 13]. Both the required force and 'apparent' storage modulus show a negligible drop for the VACNT-Si specimens, but still within experimental scatter. This could perhaps be attributed to some degradation and/or chemical erosion of specimen surface during the growth of VACNTs at an elevated 820 °C. On the other hand, damping loss factor ($\tan\delta$) shows a remarkable increase of 1800 % for the samples with VACNTs grown on pure Si wafer (Figures 3(e) and 3(f)). Interfacial friction between individual VACNTs (with very large surface area to diameter), caused by their entanglements under cyclic deformation, is believed to be the primary energy dissipation mechanism for such high improvement in loss factor [20].



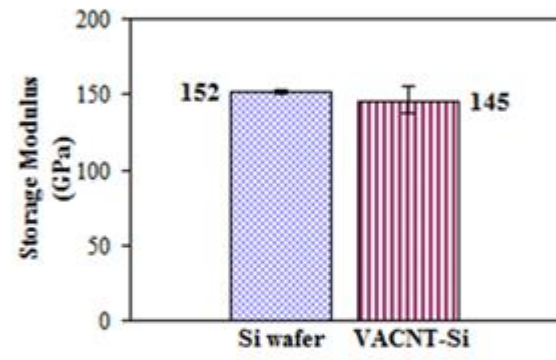
(a)



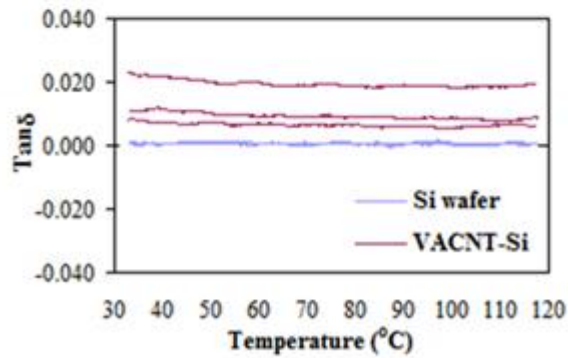
(b)



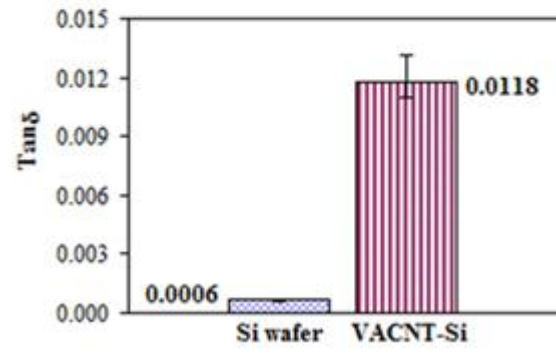
(c)



(d)



(e)



(f)

Figure 3: DMA results for three specimens each of pure Si wafer and VACNT-Si (processed at 820 °C) analyzed over a temperature range from ambient (30 °C) to 120 °C; ((a) and (b)) the required line force F at mid-span to achieve 10 μm amplitude; ((c) and (d)) the 'apparent' storage modulus, E' ; and ((e) and (f)) associated damping loss factor, $\tan\delta$ [20].

3.1.2 SHPB Response of VACNT-Si Specimens The combination of soft VACNT forest layer with hard Silicon wafer presented novel challenges for SHPB testing. The VACNT forest layer is typical of an open-cell foam structure consisting of well arranged one-dimensional units [17]. Various energy absorption mechanisms such as localized higher mode buckling of VACNTs under static compressive loading and nano-indentation along with surface entanglement and vander-walls interactions with neighboring nanotubes have been reported in literature [18, 19]. To the authors' knowledge, this type of layered material combination with such a contrast in properties has not been tested using SHPB [21] for analyzing the high strain-rate dynamic response.

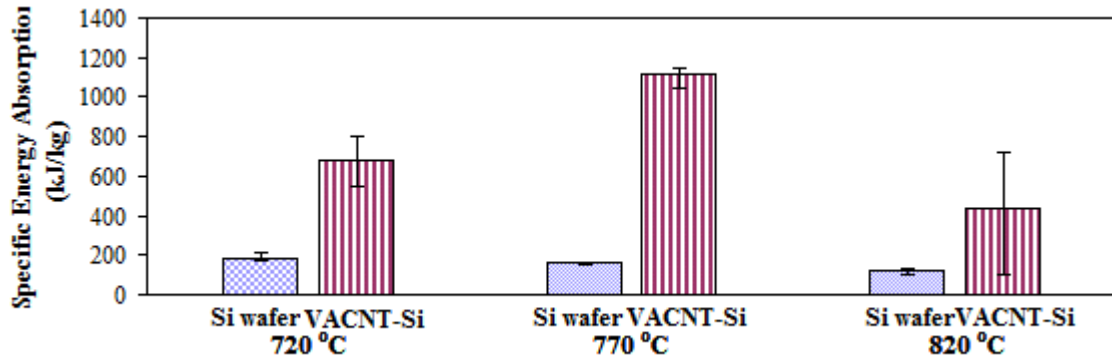


Figure 4: Specific energy absorption of pure Si-wafer and VACNT-Si (processed at 720 °C, 770 °C and 820 °C) [21].

It was once again observed that the VACNT-Si specimens processed at 770 °C and 820 °C showed a larger increase in specific energy absorption (Figure 4) compared with those processed at 720 °C. It was concluded that around 770 °C may be the optimal processing temperature for attaining the highest damping and specific energy absorption, in terms of height and alignment/entanglement of the VACNTs grown on Si-wafer substrate [21].

3.2.1 DMA Response of Woven fiber-glass Composites with Embedded VACNT Layers: The DMA experiments were conducted on FG/PE, FG/PU, FG/PE/VACNT, and FG/PU/VACNT samples (three samples each) to investigate the effects of embedded VACNT layers on specimens' dynamic mechanical behavior. The graphs for the storage modulus (flexural stiffness), loss modulus (energy dissipation), and damping loss factor ($\tan \delta$, ratio of dissipated energy to stored energy) for FG/PE and FG/PE/VACNT specimens are presented in Figure 5. As can be seen, at room temperature (RT) FG/PE/VACNT samples exhibited 40% drop in storage modulus compared to the baseline FG/PE samples. The $\tan \delta$ of FG/PE/VACNT specimens over the test temperature range from 32° C to 200° C (or frequency, by the time-temperature correspondence principle for viscoelastic materials) appeared to be consistently higher (by about 60%), but it was found to be similar as baseline FG/PE at T_g (120° C). The loss modulus of FG/PE/VACNT was higher at RT compared to the baseline FG/PE, but it was much lower at T_g (120° C). The average bulk density of FG/PE/VACNT was slightly lower than the FG/PE specimens. Glass transition temperature was almost same for both composites (120° C).

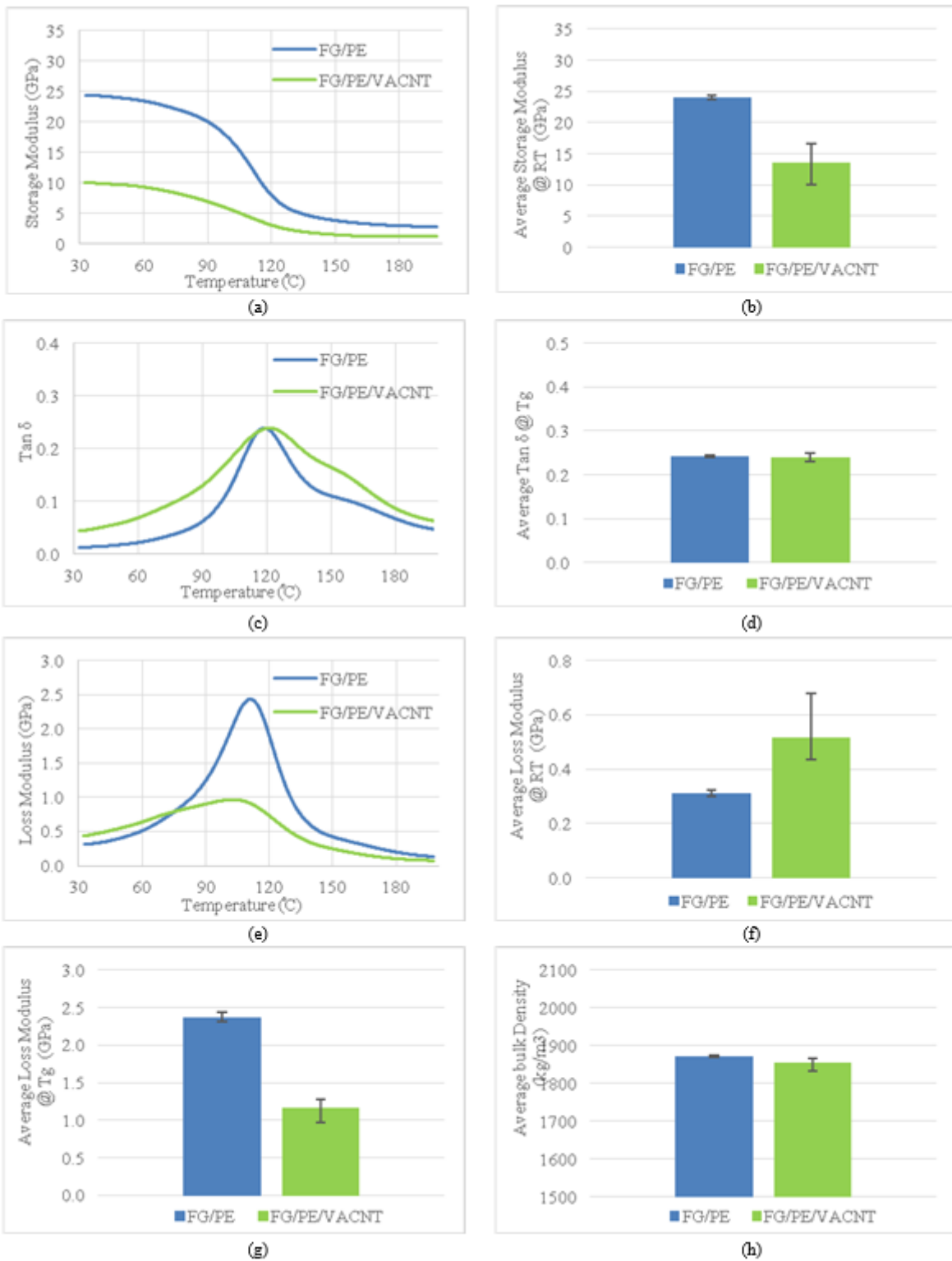


Figure 5: DMA response of 10 layer woven fiber-glass with PE resin (FG/PE), and 10 layer woven fiber-glass with PE resin along with embedded 3 layers of VACNT (FG/PE/VACNT); (a) storage modulus, (b) storage modulus at RT, (c) damping loss factor, (d) damping loss factor at T_g, (e) loss modulus, (f) loss modulus at RT, (g) loss modulus at T_g, and (h) average bulk density of specimens (three each) [12].

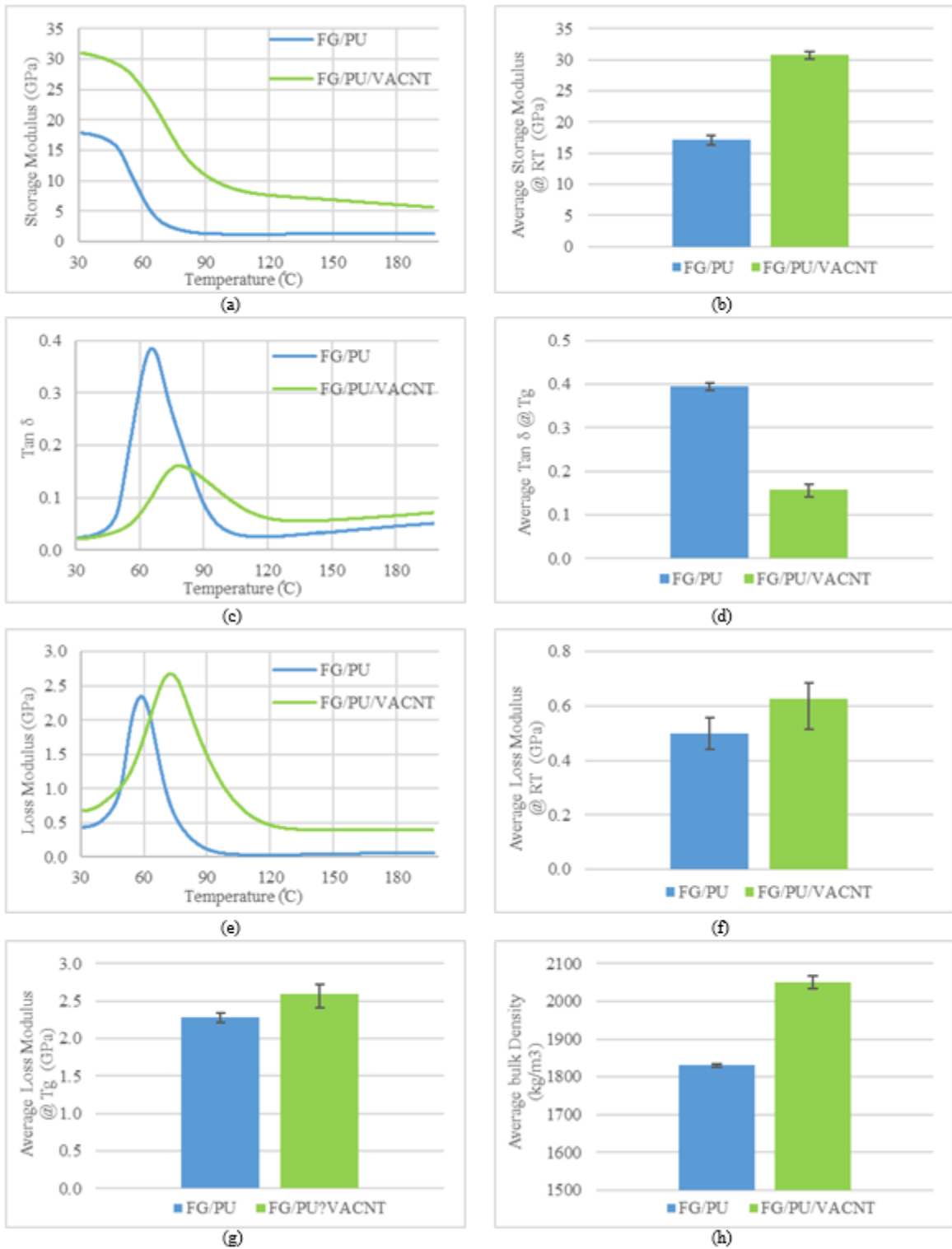


Figure 6: DMA response of 10 layer woven fiber-glass with PU resin (FG/PU), and 10 layer woven fiber-glass with PU resin along with embedded 3 layers of VACNT (FG/PU/VACNT); (a) storage modulus, (b) storage modulus at RT, (c) damping loss factor, (d) damping loss factor at T_g , (e) loss modulus, (f) loss modulus at RT, (g) loss modulus at T_g , and (h) average bulk density of specimens (three each) [12].

In Figure 6, the dynamic mechanical behavior of FG/PU/VACNT and FG/PU specimens are compared. It was found that the storage modulus of FG/PU/VACNT increased (from about 18 GPa to 31 GPa at RT) in comparison with the baseline FG/PU samples. Additionally, FG/PU/VACNT exhibited higher loss modulus both at RT and T_g . The average bulk density and T_g also increased. However, a significant drop in inherent damping ($\tan \delta$) was observed at T_g with the addition of VACNT layers (FG/PU/VACNT). In contrast to previous investigation of VACNT grown on silicon wafer substrate [20], the addition of VACNT layers did not show an increase in damping loss factor ($\tan \delta$) in FG/PE/VACNT and FG/PU/VACNT samples. However, a significant drop in damping has been observed in FG/PU/VACNT samples. The hand lay-up with subsequent pressurization of the green samples may be the major factor in reduction of damping. Increased binding of the polymers with the VACNT surface under pressure may also be contributing to the reduced damping.

3.2.2 SHPB Response of Woven fiber-glass Composites with Embedded VACNT Layers: The compression SHPB apparatus was used to evaluate the energy absorption characteristics of FG/PE, FG/PU, FG/PE/VACNT, and FG/PU/VACNT specimens. A typical SHPB compression response for FG/PE and FG/PE/VACNT specimens at strain rate of 700 to 800 /s is shown in Figure 7. FG/PE/VACNT displayed higher specific energy absorption and rate of specific energy compared to the baseline FG/PE. However, compressive strength in FG/PE/VACNT was marginally lower than baseline FG/PE.

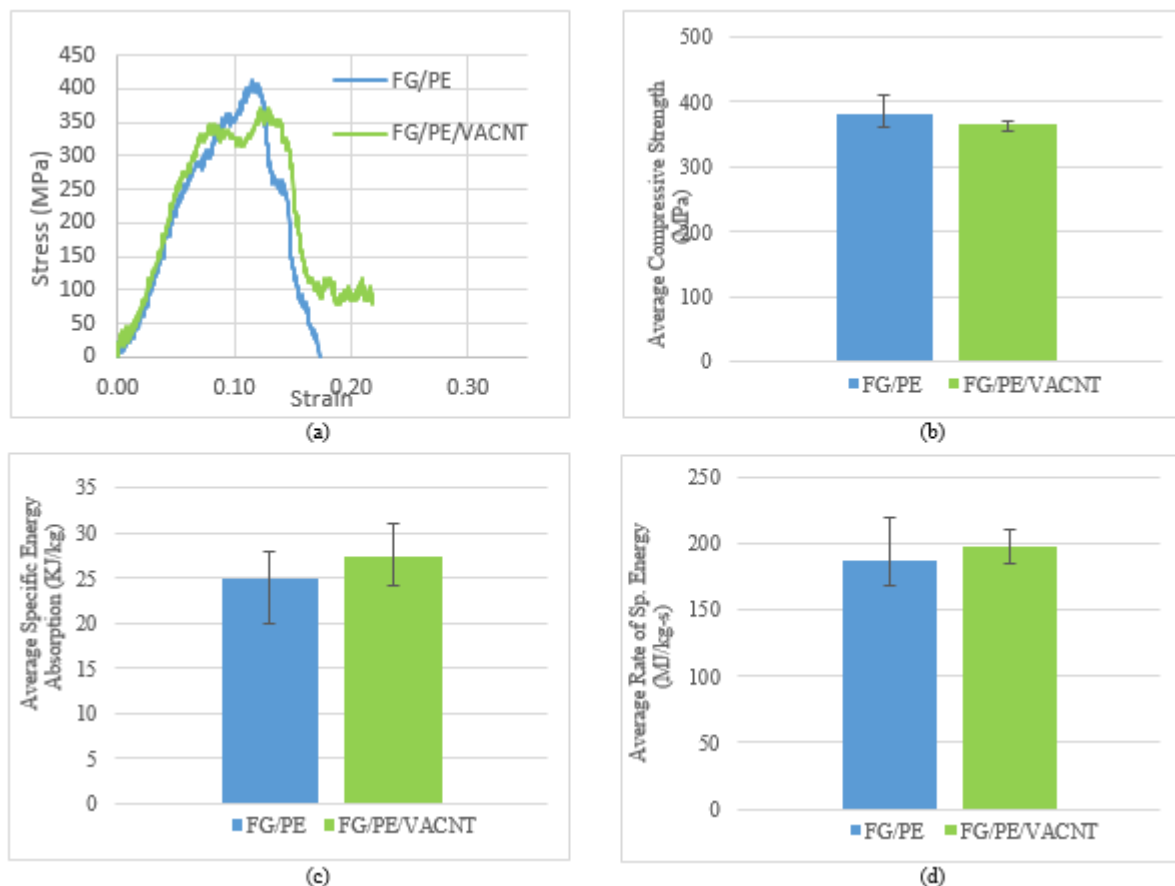


Figure 7: SHPB compression test response of FG/PE and FG/PE/VACNT composites evaluated over strain rate of 700 to 800 /s; (a) stress-strain curve of FG/PE and FG/PE/VACNT, (b) compressive strength, (c) average specific energy absorption, and (d) rate of specific energy absorption [12].

SHPB compression tests were also performed on baseline FG/PU and FG/PU/VACNT specimens at strain rate of 600 to 800 /s. Figure 8 shows typical stress-strain response of FG/PU and FG/PU/VACNT, and compares them in terms of average compressive strength, specific energy absorption, and rate of specific energy. FG/PU/VACNT exhibited higher specific energy absorption and rate of specific energy with respect to the baseline FG/PU. It was also found that the average compressive strength of FG/PU/VACNT increased about 30 % (from 214 MPa to 270 MPa) with respect to FG/PU.

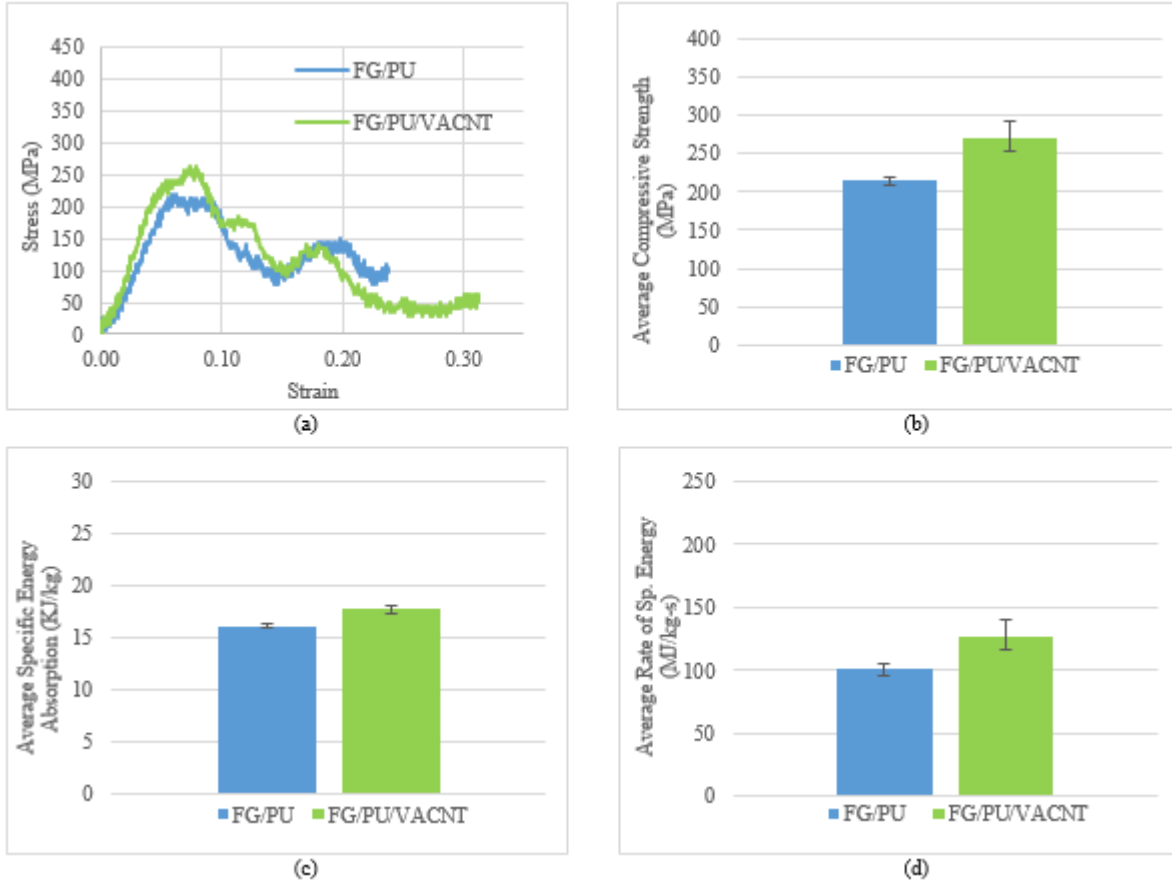


Figure 8: SHPB compression test response of FG/PU and FG/PU/VACNT composites evaluated over strain rate of 700 to 800 /s; (a) stress-strain curve of FG/PU and FG/PU/VACNT, (b) compressive strength, (c) average specific energy absorption, and (d) rate of specific energy absorption [12].

4 Conclusion

4.1 *VACNT-Si*: The dynamic mechanical behavior and high-strain rate dynamic response characteristics of a functionally graded material system consisting of vertically aligned carbon nanotube ensembles grown on a silicon wafer substrate (VACNT-Si), have been investigated. The functionally graded VACNT-Si exhibited significantly higher damping without sacrificing the flexural rigidity. Interfacial friction between individual VACNTs caused by their entanglements under cyclic deformation is believed to be the primary energy dissipation mechanism for such a large improvement in loss factor. In the case of high strain-rate compressive loading, a large increase in the specific energy absorption was observed for VACNT-Si layered specimens, as compared with pure Si wafer.

4.2 *Woven fiber-glass Composites with Embedded VACNT Layers*: Dynamic mechanical behavior and energy absorption characteristics of 10 layer woven fiber-glass fabric with two different resin systems (PE

and PU) have been investigated as the baseline; and effects of embedding VACNT layers within these baseline composites were studied. From DMA response, FG/PE/VACNT exhibited a significantly lower flexural stiffness at ambient temperature along with higher damping loss factor over the investigated temperature range with respect to baseline FG/PE. However damping loss factor was found to be similar as the baseline FG/PE at T_g . FG/PU/VACNT showed a significantly higher flexural stiffness at ambient temperature along with lower damping loss factor over the investigated temperature range compared to the baseline FG/PU. The loss modulus at RT increased with the addition of VACNT forest layers in both baseline composites (FG/PE and FG/PU), but only FG/PU/VACNT showed an increased loss modulus at T_g . From SHPB response, FG/PE/VACNT and FG/PU/VACNT showed improved specific energy absorption and rate of specific energy absorption compared to the baseline FG/PE and FG/PU. Compressive strength of FG/PU/VACNT increased by about 30 % with the addition of VACNT forest layers.

ACKNOWLEDGEMENT

The financial support from the US Army Engineer Research and Development Center-Construction Engineering Research Laboratory (ERDC-CERL), Champaign, IL, USA grant W9132T-12-P0057 is gratefully acknowledged. The authors would like to thank Dr. Matthew Brenner and Dr. Jignesh Patel for sample preparation/fabrication; and Dr. Brahma Pramanik, Dr. Tezeswi Tadepalli, Mr. Kiyun Kim, Mr. Soheil Drayadel for their help in performing the DMA and SHPB experiments.

Distribution A: Approved for public release; distribution is unlimited.

REFERENCES

- [1] Finegan, Ioana C., and Ronald F. Gibson. "Recent Research on Enhancement of Damping in Polymer Composites." *Composite Structures* 44.2-3 (1999): 89-98 (doi:10.1016/S0263-8223(98)00073-7).
- [2] Mahamood RM, Akinlabi ET, Shukla M, Pityana S: Functionally Graded Material: An Overview. Proceedings of the World Congress on Engineering 2012 Vol IIIWCE. London, UK; 2012, 3:1593-1597
- [3] Thomopoulos S, Genin GM, Birman V, editors. 2013. Structural interfaces and attachments in biology. New York: Springer. 386 p.
- [4] Ajayan, Pulickel M., and James M. Tour. "Materials science: nanotube composites." *Nature* 447.7148 (2007): 1066-1068 (doi:10.1038/4471066a).
- [5] Coleman, Jonathan N., Umar Khan, Werner J. Blau, and Yurii K. Gun'Ko. "Small but Strong: A Review of the Mechanical Properties of Carbon Nanotube-polymer Composites." *Carbon* 44.9 (2006): 1624-652 (doi:10.1016/j.carbon.2006.02.038).
- [6] Thostenson, Erik T., Zhifeng Ren, and Tsu-Wei Chou. "Advances in the Science and Technology of Carbon Nanotubes and Their Composites: A Review." *Composites Science and Technology* 61.13 (2001): 1899-912 (doi:10.1016/S0266-3538(01)00094-X).
- [7] Zeng, You, Lijie Ci, Brent J. Carey, Robert Vajtai, and Pulickel M. Ajayan. "Design and Reinforcement: Vertically Aligned Carbon Nanotube-Based Sandwich Composites." *ACS Nano* 4.11 (2010): 6798-6804 (doi: 10.1021/nn101650p).
- [8] C. M. Seah, S. P. Chai, and A. R. Mohamed, "Synthesis of aligned carbon nanotubes," *Carbon*, vol 49, pp. 4613-4635, 2011 (doi:10.1016/j.carbon.2011.06.090).
- [9] Y.J. Jung, K. Wei, P.M. Ajayan, Y. Homma, K. Prabhakaran, "Mechanism of selective growth of carbon nanotubes on SiO₂/Si patterns, *Nano Lett.*, vol 3. No 4., pp. 561-564, 2003 (doi: 10.1021/nl034075n).

- [10] C. Daraio, V. F. Nesterenko, and S. Jin, "Highly Nonlinear Contact Interaction and Dynamic Energy Dissipation by Forest of Carbon Nanotubes," *Applied Physics Letters*, vol. 85, pp.5724-5726, 2004 (<http://dx.doi.org/10.1063/1.1829778>).
- [11] S. Hinduja, S. P. Singh, P. Srivatsava, V.D. Vankar, "Growth of long aligned carbon nanotubes on amorphous hydrogenated silicon nitride by thermal chemical vapor deposition," *Mater. Lett.* vol. 63 no. 15, pp.1249-1259, 2009 (doi:10.1016/j.matlet.2009.02.050).
- [12] Kiyun Kim, *Dynamic Mechanical Analysis and High Strain-rate Energy Absorption Characteristics of Vertically Aligned Carbon Nanotube (VACNT) Reinforced Woven Fiber-glass Composites*, M.S. thesis (2015): The University of Mississippi, University, MS, USA.
- [13] B. Pramanik and P. R. Mantena, "Viscoelastic Response of Graphite Platelet and CTBN Reinforced Vinyl Ester Nanocomposites," *Materials Sciences and Applications*, vol. 2, no. 11, pp. 1667-1674, 2011 (doi 10.4236/msa.2011.211222).
- [14] TA Instruments. (2010). Q800 Dynamic Mechanical Analysis Brochure. Retrieved from <http://www.tainstruments.com/pdf/brochure/dma.pdf>.
- [15] U.S. Army Engineer Research and Development Center—Construction Engineering Research Laboratory (ERDC-CERL), Champaign, IL 61821, USA.
- [16] Chen, Weinong W., and Bo Song. *Split Hopkinson (Kolsky) Bar: Design, Testing and Applications*. New York: Springer, 2011.
- [17] A. Cao, P.L. Dickrell , W.G. Sawyer , M.N. Ghasemi-Nejhad , P.M. Ajayan , "Super-compressible foamlike carbon nanotube films", 2005 Nov 25; 310(5752):1307-10 (doi: 10.1126/science.1118957).
- [18] T. Tong, Y. Zhao, L. Delzeit, M. Ali Kashani, Meyyappan and A. Majumdar, "Height Independent Compressive Modulus of Vertically Aligned Carbon Nanotube Arrays", *Nano Letters*, Vol. 8, No. 2, 511-515, 2008 (doi: 10.1021/nl072709a).
- [19] S. B. Hutchens, A. Needleman, J. R. Greer, Analysis of uniaxial compression of vertically aligned carbon nanotubes, *Journal of the Mechanics and Physics of Solids*, 59 (2011) 2227–2237 (doi:10.1016/j.jmps.2011.05.002).
- [20] Mantena, P. Raju, Tezeswi Tadepalli, Brahmananda Pramanik, Veera M. Boddu, Matthew W. Brenner, L. David Stephenson, and Ashok Kumar. "Energy Dissipation and the High-Strain Rate Dynamic Response of Vertically Aligned Carbon Nanotube Ensembles Grown on Silicon Wafer Substrate." *Journal of Nanomaterials* 2013 (<http://dx.doi.org/10.1155/2013/259458>).
- [21] Mantena, P. Raju, Brahmananda Pramanik, Tezeswi Tadepalli, Veera M. Boddu, and Matthew W. Brenner. "Effect of Precess Parameters on the Dynamic Modulus, Damping and Energy Absorption of Vertically Aligned Carbon Nano-Tube (VACNT) Forest Structures." *Journal of Multifunctional Composites* (2014): 93-100 (doi:10.12783/issn. 2168-4286/2.2/Mantena).